

Floating binary planets from ejections during close stellar encounters

Yihan Wang^{1,3*†}, Rosalba Perna^{2,4†} and Zhaohuan Zhu^{1,3}

^{1*}Nevada Center for Astrophysics, University of Nevada, 4505 S. Maryland Pkwy., Las Vegas, 89154, NV, USA.

²Department of Physics and Astronomy, Stony Brook University, 100 Nichols road, Stony Brook, 11794, NY, USA.

³Department of Physics and Astronomy, University of Nevada, 505 S. Maryland Pkwy., Las Vegas, 89154, NV, USA.

⁴Center for Computational Astrophysics, Flatiron Institute, 162 5Th Ave, New York, 10010, NY, USA.

*Corresponding author(s). E-mail(s): yihan.wang@unlv.edu;
 Contributing authors: rosalba.perna@stonybrook.edu;
zhaohuan.zhu@unlv.edu;

†These authors contributed equally to this work.

Abstract

The discovery of planetary systems beyond our solar system has posed challenges to established theories of planetary formation. Planetary orbits display a variety of architectures not predicted by first principles, and free-floating planets appear ubiquitous. The recent discovery of candidate Jupiter Mass Binary Objects (JuMBOs) by the *James Webb Space Telescope (JWST)* further expanded this enigma. Here, by means of high-accuracy, direct N -body simulations, we evaluate the possibility that JuMBOs may form as a result of ejection after a close stellar flyby. We consider a system of two Jupiter-like planets moving in circular orbits with velocities \mathbf{v}_1 and \mathbf{v}_2 at distances \mathbf{a}_1 and \mathbf{a}_2 around a Sun-like star. The interloper is another Sun-like star approaching with asymptotic velocity \mathbf{v}_∞ . We find that JuMBOs can indeed be formed upon ejection if the two planets are nearly aligned as the interloper reaches the closest approach. The ratio of the cross section of JuMBOs production to that of single ejected free-floating planets can approach $\sim 20\%$ for $v_\infty/v_2 \sim 0.1 - 0.2$ and $a_1/a_2 \sim 0.65 - 0.7$. JuMBOs formed via this channel are expected to have an average semi-major axis comparable to $\Delta a \sim 3(a_2 - a_1)$ and high eccentricity, with a distinctive superthermal

distribution which can help to observationally identify this formation channel and distinguish it from primordial formation. We determine an upper limit on the JuMBO formation efficiency per planetary system, assuming a minimum of two orbiting giants. In very dense star clusters like the Trapezium in the Orion Nebula, this efficiency can reach several tens of percent. If the ejection channel is confirmed for these or future *JWST* observations, these JuMBOs will directly inform us of the conditions where these giant planets formed in protoplanetary disks, putting stringent constraints on the giant planet formation theory.

Keywords: planetary systems, simulations, dynamics

The discovery and investigation of over 4,000 exoplanets beyond our Solar System has unveiled a remarkable variety of exoplanets and shown that our own planetary system is far from typical [1]. Particularly, the discovered giant planets turn out to be the most puzzling population, challenging the conventional theory of giant planet formation.

In the conventional core accretion theory, a solid core is first assembled through planetesimal accretion [2] or pebble accretion [3, 4]. As the core’s gravity becomes strong, a hydrogen-helium gaseous envelope starts to develop around the planetary core. This envelope accretion phase is the longest stage of giant planet formation due to the envelope’s slow Kelvin-Helmholtz contraction. If the envelope mass could eventually reach the core mass within the disk lifetime, the envelope would accrete exponentially, and the planet would enter the runaway stage to become a full-grown giant planet. With nominal disk parameters, the core mass needs to be $\gtrsim 10M_{\oplus}$ for runaway to occur before the gaseous disk dissipates within about ~ 3 Myrs. The ice particles beyond the frost line help supply additional solids to build this massive core.

Although this conventional model could explain our solar system, it meets some challenges in explaining giant exoplanets. As a start, the ‘hot Jupiters’, the first discovered exoplanets around main-sequence stars [5], are found to be situated remarkably close to their host stars, well within the frost line. Second, many of these ‘hot Jupiters’ inhabit highly eccentric orbits and display significant relative inclinations [6], at odds with the circular co-planar orbits of giant planets in our own solar system. Third, the recent detection of giant planets orbiting low-mass stars [7] suggests efficient giant planet formation, defying the core accretion theory. Fourth, this theory is further questioned by the observation of brown dwarfs/planets on extremely wide orbits, larger than ~ 100 AU [8] and even up to 10^6 AU [9]. Finally, the presence of floating planets has also been another puzzle for this theory [10]. Very recently, the mystery has deepened with the discovery by the *James Webb Space Telescope (JWST)* [11] that a fraction of these floating planets, largely Jupiter-like giants, is moving in a couple, thus making up a new population of binary planets whose existence does not readily fit in any current planetary formation theory. Although some of these challenges can be remedied by invoking additional physical processes (e.g., planet migration [12], planet-star tidal interaction [13], planet-planet scattering [14], more realistic disk physics [15]), most of these processes could only operate for planets whose semi-major axes

are within several AU. It is still challenging to explain giant planets far away from the star [16], and the abundant free-floating planets, using the core accretion theory.

On the other hand, the alternative theory of giant planet formation, the disk gravitational instability model [17], can form giant planets efficiently beyond 50 AU. When young protoplanetary disks are massive enough, they are subject to gravitational instability and develop spiral arms. If disk cooling is fast enough, these spirals can fragment and collapse to giant planets directly [18]. With typical protoplanetary disk conditions, this fast cooling can be achieved beyond 50 AU [19]. The clumps collapse quickly and form planets with several Jupiter masses. Although this theory has its own challenges, particularly in explaining terrestrial planets close to the star (but see [20, 21]), it can form multiple giant planets efficiently beyond 50 AU at early disk evolutionary stages [22].

It is difficult to test these two formation models using mature exoplanets that are billions of years old. It is crucial to discover young giant planets. Unfortunately, we only have a few candidates discovered in protoplanetary disks (e.g. PDS 70bc at 21 and 34 AU from the central star [23, 24]). Very recently, a large number of free-floating planets has been discovered in young stellar associations [10], which offers a new opportunity to constrain planet formation theories. Intriguingly, a promising avenue of exploration has emerged that ventures beyond intrinsic mechanisms—namely, the influence of external perturbations on planetary architectures (e.g. [25–42]). Planetary systems are in fact likely born in young star clusters. In such dense stellar environments, frequent gravitational interactions between celestial objects become commonplace, potentially reshaping planetary systems over time. This dynamic interplay in crowded clusters offers an alternative perspective on planetary formation and the planet orbital configurations at early formation times, addressing some of the existing gaps in our understanding.

This work has been motivated by the very recent report of *JWST* observations of candidate Jupiter-Mass Binary Objects (a.k.a. JuMBOs) which are also quite young [11]. More specifically, via dedicated N -body simulations, we set to investigate the possibility that a close flyby can result in the ejection of two planets in outer orbits, which then remain bound to one another. While the initial motivation for this exploration came from the observations mentioned above, our simulations robustly demonstrate that JuMBO formation is actually an *unavoidable* outcome of close-by interactions in dense stellar environments, and the properties of JuMBOs are directly related to their initial configurations in protoplanetary disks. We quantify their occurrence as a function of the type of stellar environment and the original planetary configuration and make predictions for their properties which can be tested with future *JWST* observations.

1 Results

Our planetary system consists of two equal-mass planets with mass m in circular orbits with semi-major axes a_1 and a_2 , and a host star with mass M_1 . Both planets move in circular orbits around the host star with initial phases ν_1 and ν_2 with respect to the X axis, and velocities v_1 and v_2 corresponding to the orbital semi-major axes

(SMA) a_1 and a_2 , respectively. The flyby intruder with mass M_2 approaches the planetary system with impact parameter b and asymptotic velocity at infinity v_∞ . We assume the orientation of the planetary system to be isotropically distributed, which translates into the parameter distributions $\cos I \in [-1, 1]$ and $\Omega \in [0, 2\pi]$, where I is the orbital inclination, and Ω is the longitude of the ascending node. The schematics of the scattering experiment, with all the variables involved, are shown in Fig. 1. Throughout the paper, we adopt a generic (fixed) mass ratio $m/M_1 = 10^{-3}$ (similar to the mass ratio between Jupiter and the Sun), and $M_2/M_1 = 1$ for simplicity. We ran 10^8 scattering experiments for each combination of $(v_\infty/v_2, a_1/a_2)$ and found that JuMBO form as an outcome of ejection following the flyby, especially if the two giant planets are nearly aligned when the intruder is at its closest approach. We explore and quantify their properties in the following.

We begin by investigating the dependence of the relevant JuMBO properties on the angles I and Ω . This is shown in Fig. 2 for a fixed value $a_1/a_2 = 0.7$ and three choices of v_∞/v_2 . From top to bottom, we show the relative cross section (normalized to the maximum value) of JuMBO formation, the semi-major axis (SMA) of the JuMBO normalized to $\Delta a = (a_2 - a_1)$, and the eccentricity. A notable characteristic of the cross section for JuMBO formation is the highest probability for edge-on scatterings when either Ω or I is 0 or π (symmetry exists with respect to these values as $\theta \in [0, 2\pi]$). In contrast, the probability is lowest for face-on scatterings where $\Omega = I = \pi/2$. During face-on scatterings, the interloper interacts with the planetary system for a relatively short duration as it crosses the planetary orbital plane. However, in edge-on scatterings, the interloper interacts with the planetary system for a much longer time as it travels along the orbital plane. This is especially true for prograde edge-on scatterings, where the interloper and the two planets move in the same direction. Their minimal relative velocity increases the interacting time, leading to a higher chance of ejecting two giant planets consecutively.

The semi-major axis (SMA) of a JuMBO is highest when the scattering is close to face-on and lowest when the scattering is edge-on. JuMBOs tend to form when the two giant planets are nearly aligned as the intruder approaches its closest point. At this time, their separation upon ejection is approximately equal to the difference in their SMA, and their relative velocity difference aligns closely with their Kepler velocity difference. In edge-on scatterings, the intruder imparts momentum parallel to the planets' velocities. The outer planet, which has a lower Keplerian velocity, gains more momentum since it's closer to the intruder. In contrast, the inner planet gains relatively less momentum due to its greater distance from the intruder. Consequently, the intruder tends to decrease their relative velocity upon ejection. For face-on scatterings, the imparted momentum is perpendicular to the Keplerian velocities of the two planets. This results in a weaker relative velocity reduction compared to edge-on scatterings. A smaller relative velocity upon ejection results in a smaller binding energy post ejection, leading to a decreased SMA as indicated by Eq 3. Due to the reduction in relative velocity, the eccentricity of the JuMBOs tends to be very high, stemming from the small angular momentum between the two ejecting planets. Edge-on scatterings are more efficient at reducing this relative velocity, which is why we observe JuMBOs with higher eccentricities resulting from these scatterings.

Fig. 3 compares the cross sections for ejection of a single planet (top panel) with that of JuMBOs (bottom left panel). As expected, both are favored by lower relative velocities of the flyby star. However, while the ejection of a single planet is largely independent of the relative initial orbits of the two planets, the probability of ejection of JuMBOs increases as the two planets are initially in more closely spaced orbits. This becomes more apparent in the ratio between the cross sections, which is shown in the bottom right panel of Fig. 3.

To relate our dimensional outcomes to direct astrophysical environments, the figures explicitly indicate with vertical lines the location of the ratio v_∞/v_2 for an outer planet at $a_2 = 10$ AU (in blue) and at $a_2 = 100$ AU (in red), each for three values of the velocity dispersion, $\sigma_v = 1, 5, 10$ km/s, roughly corresponding to the typical values encountered in open clusters, globular clusters, and OB associations, respectively. Smaller clusters are more conducive to JuMBO formation. Since the production probability is larger for smaller values of v_∞/v_2 , planets in wider orbits require smaller clusters/velocity dispersion in order to be ejected and form JuMBOs.

The orbital properties of the dynamically-formed JuMBOs are displayed in Fig. 4, with the top panels showing the mean and standard deviation (STD) of the SMA, and the bottom panels displaying the same quantities for the eccentricity. The general features of this JuMBO population are a large eccentricity, mostly in the range of $e_{\text{JuMBO}} \sim 0.65 - 0.75$, with a standard deviation ~ 0.3 . The mean of the semi-major axis a_{JuMBO} has a spread of a few around Δa , with an STD also of a few. As intuitively expected, tighter binaries are formed for initially closer separations between the two planets.

Last, we compute and show in Fig. 5 the probability density function (PDE) for the SMA (left panel) and the eccentricity (right panel) of the JuMBOs, for four representative values of v_∞/v_2 and the value of $a_1/a_2 = 0.7$, which is in the region where the JuMBO probability production is the highest. These PDEs hence represent the distributions that observations of JuMBOs formed via ejection would be seeing. It has been demonstrated that in the fast scattering regime, where $v_\infty/v_2 \gg 1$, the SMA distributions exhibit distinctive shapes[43–45]. Since the two planets in a JuMBO are nearly aligned upon ejection, the intruder imparts less momentum to the planets in the fast scattering regime than in the slow scattering regime. This is attributed to the relatively shorter interaction time in the fast scattering regime. As a result, the reduction in relative velocity as discussed above is less efficient in a fast scattering interaction. Consequently, achieving a smaller SMA for the JuMBO is more challenging in the fast scattering regime.

We further observe that, while the PDE of a_{JuMBO} is peaking around the value $\sim 3(a_2 - a_1)$, it has however a broad tail at larger values. Hence forming JuMBOs with large SMA is natural within the mechanism of our study. Planets at very large separation are known to exist [9], while more typical outer planets at tens of AU can easily form JuMBO with SMA in the 100s AU range. However, if a large sample of observations shows that the JuMBO distribution is very heavily dominated by wide binaries, with $a_{\text{JuMBO}} \gtrsim 100$ AU (as suggested by the first set of JuMBO candidates [11]), then the JuMBO formation mechanism identified in this work would support

the giant planet formation models that can efficiently produce wide-orbit giant planets in young protoplanetary disks, e.g. the disk gravitational instability model [17]. Meanwhile, the two planet formation models are not mutually exclusive, and the giant planet population at $\lesssim 10$ AU could still form through core accretion at later disk evolutionary stages.

The JuMBO eccentricity distribution is found to be superthermal, as can be seen in the right panel of Fig. 5 as compared to the thermal distribution. This is a very distinctive feature of our JuMBO formation mechanism since the eccentricity distribution expected in scenarios of primordial formation from Interstellar Medium (ISM) clouds is expected to be subthermal [46, 47].

The absolute rate of JuMBO formation is dependent on the stellar density in the interacting cluster, which, in virialized systems, can be determined from their mass and velocity dispersion. However, it is also dependent on the highly uncertain fraction of planetary systems with giant planets in outer orbits, which hence makes a numerical evaluation of the absolute rate rather approximate at this stage. Nonetheless, using the formalism of rate calculation detailed in Sec.4.2 of the Methods, we can make an estimate for the number of JuMBOs produced via our proposed mechanism. In particular, in the optimal scenario where every planetary system contains at least two giant planets, we can derive an upper limit for the JuMBO production efficiency per planetary system, as a function of a_1 and a_2 .

The left panel of Fig 6 displays the magnitude of this upper limit for the specific case of the inner Trapezium region of the Orion Nebula Cluster (ONC) over 1 Myr, assuming $1 M_\odot$ for the stellar masses, and $1 M_J$ for the giant planet masses. It is evident that a significant number of JuMBOs can be produced in the ONC for wide planetary systems with closely paired giant planets, enabled by stellar flybys. In particular, the observations by [11] revealed about 40 JuMBOs for a stellar population of ~ 2000 stars, hence suggesting a production efficiency of $\sim 2\%$ per planetary system. For JuMBOs primarily exhibiting semi-major axes in the range of approximately 50 – 350 AU ([11]), such a proportion would necessitate around 10 – 20% of stars hosting giants with orbits spanning about 20–150 AU (since $a_{\text{JuMBO}} \sim 3[a_2 - a_1]$), according to the rates per planetary systems illustrated in the left panel of Fig. 6. This requirement is in line with observations, particularly for more massive stars ([48, 49]). We thus argue that JuMBO formation via ejections following stellar flybys provides a viable explanation for the reported JuMBO observations in a very dense star cluster [11].

As an useful comparison, the right panel of Fig 6 illustrates the upper limit of JuMBO production for a typical open cluster. It is evident that even in the optimal case of two wide-orbit planets for every star, the absolute JuMBO production rate remains low. Consequently, JuMBO production via this mechanism would not be a viable explanation if such objects were to be found in low-density star clusters.

2 Conclusion

Dynamical encounters in interacting stellar environments can give rise to a variety of planetary architectures which collectively would be difficult to otherwise explain via

conventional models of planetary formation. Here, via a large suite of dedicated N -body simulations, we have shown that close flybys in dense stellar clusters *unavoidably* lead to a sizeable fraction of free-floating binary planets, in addition to the already known single free-floating planets.

Our simulations have allowed us to quantify their probabilistic outcomes depending on the initial planetary properties and those of their host stellar cluster, as well as characterizing their orbital properties. JuMBOs can be produced with a wide range of semi-major axes, largely correlated with the difference between the original orbital distances of the ejected planets. Most notably, they are expected to have high eccentricity with a superthermal distribution, unlike in the primordial formation channel from ISM clouds, which predicts a sub-thermal distribution.

Recent observations with the JWST have identified some of these candidates in a very dense star cluster [11]. We have shown that JuMBO formation from ejections occurs with an efficiency which is broadly consistent with these observations. With much more data expected in the years to come, our results will allow to further test this dynamical formation scenario. A characterization of the JuMBO orbital properties, and their relative fraction with respect to that of FFJ, will allow us to probe primordial planetary architectures and thus help discriminate between competing theories of planetary formation.

3 Figures

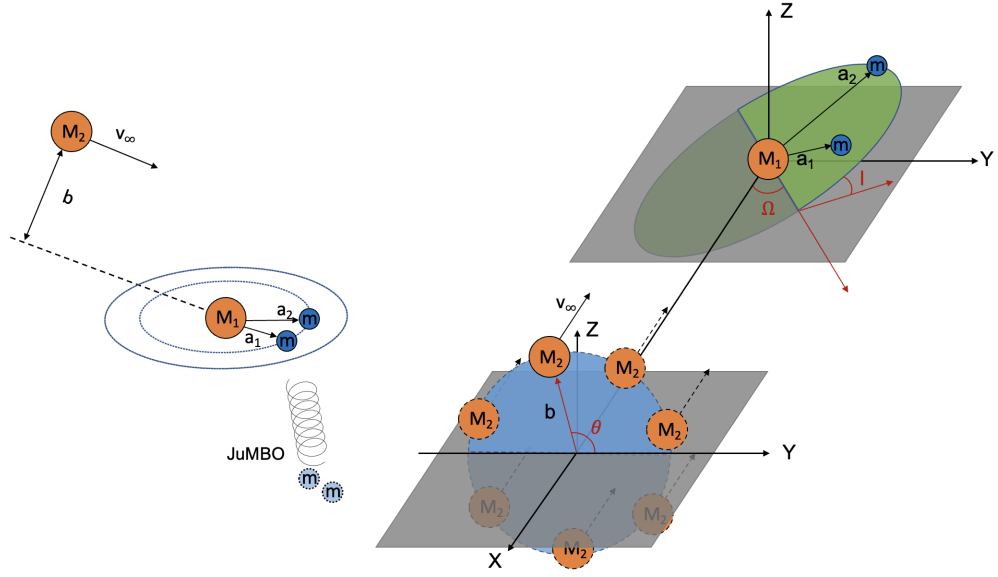


Fig. 1 *Left:* Schematics of the astrophysical scenario we explore. A close stellar flyby to a planetary system results in the ejection of two planets, which thereof remain bound, forming a floating planetary binary. *Right:* Schematics of the scattering experiments set to explore the occurrence of such a scenario. Two equal-mass, co-planar planets orbit a star of mass M_1 . An interloper star of mass M_2 flies by with asymptotic velocity v_∞ parallel to the X direction, impact parameter b and angle θ in the plane perpendicular to the direction of motion of M_2 . The planetary orbital plane forms an angle I , and is rotated by an angle Ω , with respect to the direction of motion of M_2 .

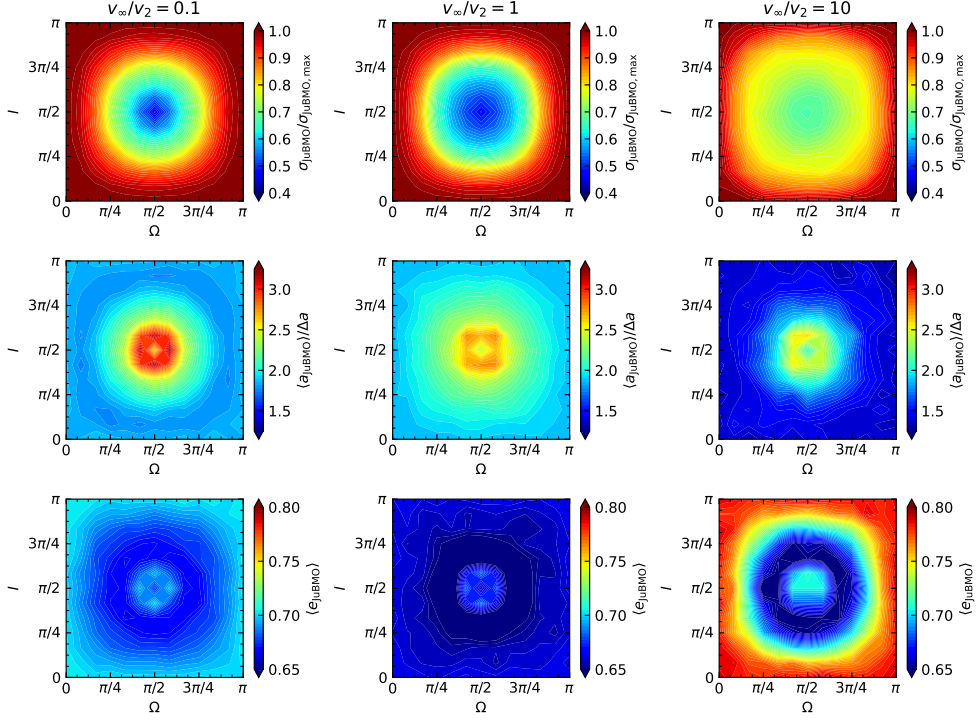


Fig. 2 Dependence on the geometry of the encounter of the differential cross section for JuMBO production (top panels), of the SMA of the JuMBO (middle panels), and their eccentricity (bottom panels). From left to right, the velocity of the scatterer is increasing. In all the cases, the initial ratio between the SMA of the two planets is $a_1/a_2 = 0.7$ while the angle $\theta \in [0, 2\pi]$.

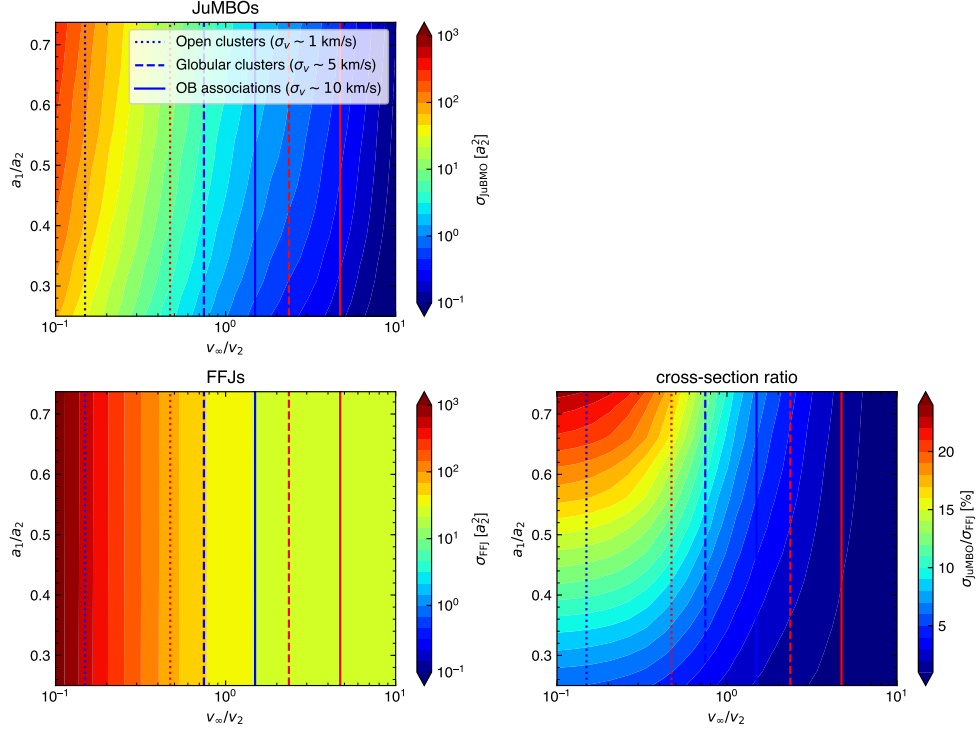


Fig. 3 Cross section for the production of JuMBOs (top panel) and FFJs (bottom left panel), as a result of ejections from their home planetary system due to a flyby. The relative cross section of JuMBO to single-floating planets is displayed in the bottom right panel. The vertical lines in all the panels show the value of v_∞/v_2 corresponding to $a_2 = 10$ AU (blue lines) and $a_2 = 100$ AU (red lines), each for the three representative dispersion velocities of the star cluster indicated in the inset of the top panel.

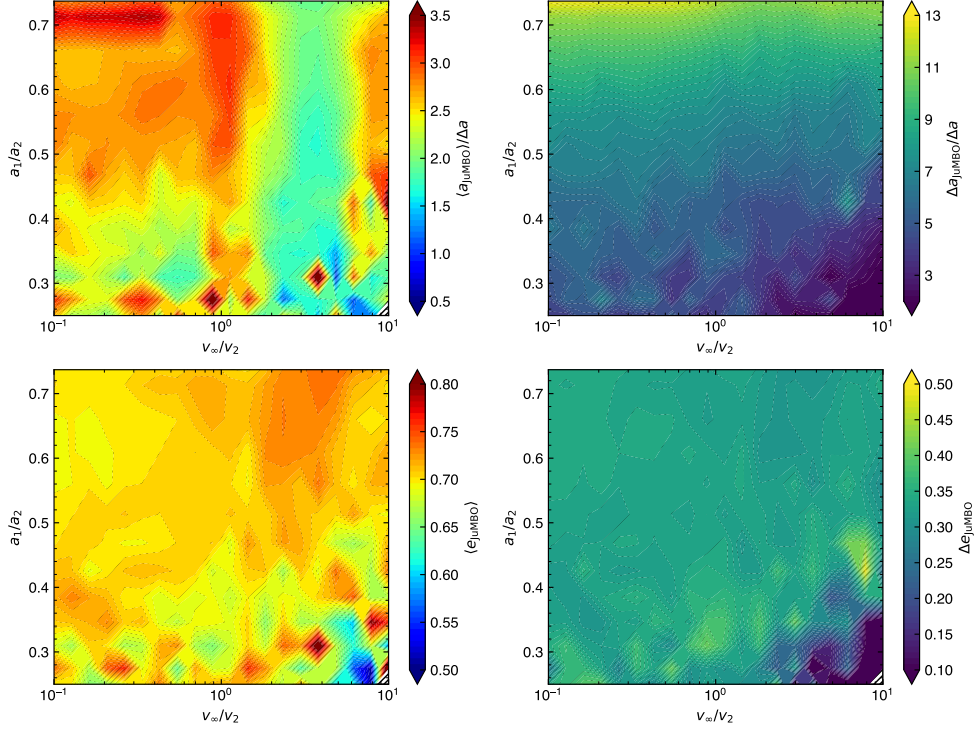


Fig. 4 Orbital parameters of the ejected JuMBO. The top panels display the mean (left panel) and the standard deviation (right panel) of the semi-major axis of the binary while the bottom panels correspondingly show the same quantities but for the eccentricity. JuMBO are expected to be eccentric and with semi-major axis comparable to Δa .

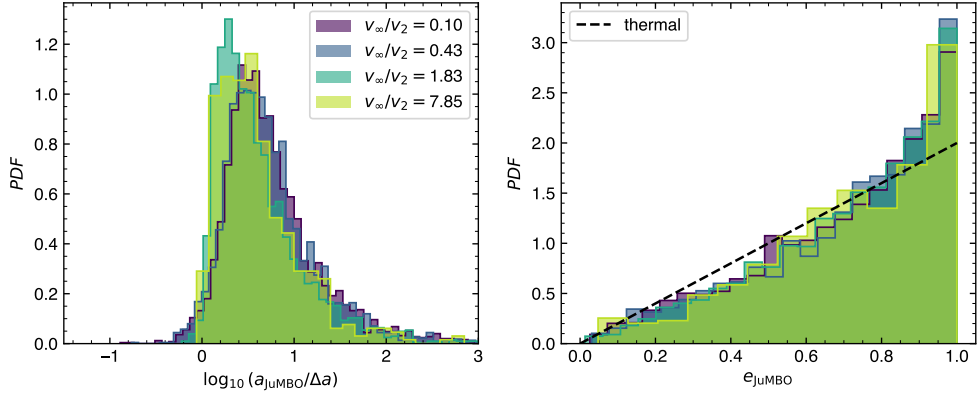


Fig. 5 The distribution of semi-major axis (left panel) and of eccentricity (right panel) of JuMBO for four values of the ratio v_∞/v_2 and $a_1/a_2 = 0.7$. Note that the former is broadly centered around $(a_2 - a_1)$, while the latter is superthermal. Such eccentricity distribution is a distinctive feature of this formation mechanism, which can observationally distinguish it from primordial formation in ISM clouds.

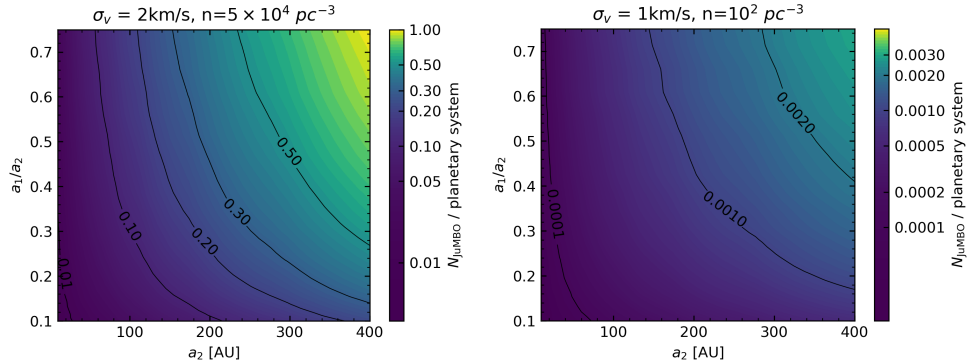


Fig. 6 Upper limit (i.e. with normalization $f_{2,J}(t=0) = 1$) for the number of JuMBOs produced per planetary system over 1 Myr due to stellar ejections, as a function of the orbital parameters a_1 and a_2 . *Left panel*: stellar density and velocity dispersion as measured in the Trapezium cluster (adopted from [50]); *Right panel*: conditions typical of an open cluster.

4 Methods

4.1 Cross-section calculation

To calculate the cross-sections of single free-floating Jupiter-mass planets (FFJs) and JuMBOs resulting from stellar flybys, we investigate the parameter space delineated by $v_\infty/v_2 \in [10^{-1}, 10]$ and $a_1/a_2 \in [0.25, f_{\max}]$ by using the high-precision N -body code Spacehub [51]. We use 20 equally spaced grids for each parameter. Here, f_{\max}

represents the maximum allowable ratio that ensures

$$a_2 - a_1 > 2\sqrt{3}R_{\text{Hill}} \sim 2\sqrt{3} \left(\frac{2m}{3M_1} \right)^{1/3} \left(\frac{a_1 + a_2}{2} \right). \quad (1)$$

This is a key condition for the two planets to remain stable prior to scattering. For each grid, we conduct 10^8 scattering experiments, ensuring a uniform distribution for $\nu_1, \nu_2, \cos I, \Omega, \theta$. M_2 is generated at asymptotic infinity within a circle of radius b_{max} ,

$$b_{\text{max}} = r_{\text{p,max}} \sqrt{1 + \frac{2G(M_1 + M_2)}{v_{\infty}^2 r_{\text{p,max}}}}, \quad (2)$$

where $r_{\text{p,max}}$ is the maximum closest approach distance, which we set to be at $5a_2$ as a conservative estimate to ensure that all FFJs and JuMBOs formed from a stellar flyby are included in the scattering outcomes.

At the end of each scattering experiment, the pairwise SMA and eccentricity between particle m_i and m_j are calculated based on their pairwise relative position \mathbf{r}_{ij} and velocity \mathbf{v}_{ij} ,

$$\frac{G(m_i + m_j)}{-2a_{ij}} = \frac{\mathbf{v}_{ij} \cdot \mathbf{v}_{ij}}{2} - \frac{G(m_i + m_j)}{r_{ij}} \quad (3)$$

$$\mathbf{e}_{ij} = \frac{\mathbf{v}_{ij} \times (\mathbf{r}_{ij} \times \mathbf{v}_{ij})}{G(m_i + m_j)} - \frac{\mathbf{r}_{ij}}{r_{ij}}, \quad (4)$$

where $r_{ij} = |\mathbf{r}_{ij}|$. If $a_{ij} > 0$, it means that particles m_i and m_j are in a bound state as a binary, provided they are not in a bound state with other particles. FFJs are characterized by planet-mass particles (denoted by m here) that are not in a bound state with any other particle. In contrast, JuMBOs are identified when two planet-size particles are in a bound state and not bound to any other particle. The duration of the scattering experiments ensures that the particles are well-separated before the scatterings are terminated.

The cross-sections of FFJ and JuMBO are respectively calculated via

$$\sigma_{\text{FFJ}} = \pi b_{\text{max}}^2 \frac{N_{\text{FFJ}}}{N} \quad (5)$$

$$\sigma_{\text{JuMBO}} = \pi b_{\text{max}}^2 \frac{N_{\text{JuMBO}}}{N}, \quad (6)$$

where N represents the total number of scatterings, N_{FFJ} denotes the number of scatterings that result in FFJ production, and N_{JuMBO} indicates the number of scatterings leading to JuMBO production.

4.2 Rate estimation

The rate of JuMBO formation per planetary system can be estimated via the equation

$$\mathcal{R}_{\text{JuMBO}} \sim f_{2J} \int n v_{\infty} \sigma_{\text{JuMBO}}(a_1, a_2, v_{\infty}) f(v_{\infty}) f(a_1, a_2) da_1 da_2 dv_{\infty}, \quad (7)$$

where f_{2J} is the fraction of planetary systems which host two Jupiter-mass planets, n is the number density of the stars, $f(v_{\infty})$ is the velocity distribution function normalized such that $\int f(v_{\infty}) dv_{\infty} = 1$, and $f(a_1, a_2)$ is the joint semi-major axis distribution function of two Jupiter mass planets that satisfy $\int f(a_1, a_2) da_1 da_2 = 1$. For thermal systems, the velocity distribution is Maxwell-Boltzmann. The joint probability functions $f(a_1, a_2)$ and f_{2J} are poorly constrained both observationally due to the observation bias toward closer planets to their host star, and theoretically due to different predictions made by different planet formation theories: while the core accretion theory (e. g. [2]) has difficulties in accounting for planets on such wide orbits, they can easily be accounted for by the disk-instability model [17].

Nonetheless, we can make generic rate predictions based on parametrizations of these uncertain functions. For a given initial $f_{2J}(t=0)$, we can assume $f(v_{\infty}) = \delta(\sigma_v)$, $f(a_1, a_2) = \delta(a_1)\delta(a_2)$ (which implies that other close encounters do not significantly modify this distribution), and thus estimate the absolute JuMBO production rate as a function of a_1 and a_2 . Here, σ_v represents the velocity dispersion of the star cluster, which has density n . With this, the number of JuMBOs produced per planetary system over a period t can be estimated by using the following equation

$$N_{\text{JuMBO}} = \int f_{2J}(t) n \sigma_v \sigma_{\text{JuMBO}} dt. \quad (8)$$

The time-dependent function $f_{2J}(t)$ is derived from the equation

$$\frac{df_{2J}}{dt} \sim -\frac{f_{2J} \sigma_{\text{FFJ}} \sigma_v}{V_c} - \frac{f_{2J} \sigma_{\text{JuMBO}} \sigma_v}{V_c} \sim -\frac{f_{2J} \sigma_{\text{FFJ}} \sigma_v}{V_c}, \quad (9)$$

where V_c represents the volume of the star cluster, and we have used the fact that $\sigma_{\text{FFJ}} \gg \sigma_{\text{JuMBO}}$. This yields the solution for f_{2J} as

$$f_{2J} = f_{2J}(0) e^{-\frac{t}{\tau_{\text{ej}}}}, \quad (10)$$

$$\tau_{\text{ej}} = \frac{V_c}{\sigma_{\text{FFJ}} \sigma_v}. \quad (11)$$

In the optimal scenario, i.e. assuming $f_{2J}(0) = 1$, we can thus derive an upper limit to the number of JuMBOs produced via ejection per planetary system over a period of time in the cluster. The results are displayed in Figure 6, where we contrast the JuMBO numbers for the Trapezium cluster ($n \sim 5 \times 10^4 \text{ pc}^{-3}$ and $\sigma_v \sim 2 \text{ km/s}$ in the inner region $< 0.2 \text{ pc}$ [50]) with those of a more typical, less dense stellar cluster ($n \sim 10^2 \text{ pc}^{-3}$ and $\sigma_v \sim 1 \text{ km/s}$).

The rate of the single FFJs can be similarly calculated as

$$\mathcal{R}_{\text{FFJ}} \sim \sum_i f_{iJ} \int n v_\infty \sigma_{\text{FFJ}}(a_1, \dots, a_i, v_\infty) f(v_\infty) dv_\infty f(a_1, \dots, a_i) da_1 \dots da_i, \quad (12)$$

where f_{iJ} is the fraction of planetary systems hosting i Jupiter-mass planets, and $\sigma_{\text{FFJ}}(a_1, \dots, a_i, v_\infty)$ represents the overall cross section of FFJ production for planetary systems with i Jupiter-mass planets. This cross section takes into account the cases of multiple single ejections, albeit it is dominated by the single ejection of the outermost planet. Observationally, f_{1J} predominates over f_{2J} , while f_{3J} and subsequent fractions are negligible.

The relative rate of JuMBO to FFJ is then given by the ratio $\mathcal{R}_{\text{FFJ}}/\mathcal{R}_{\text{JuMBO}}$, which can be approximated as

$$\frac{\mathcal{R}_{\text{JuMBO}}}{\mathcal{R}_{\text{FFJ}}} \sim \frac{f_{2J}}{f_{1J} + f_{2J}} \frac{\sigma_{\text{JuMBO}}}{\sigma_{\text{FFJ}}}. \quad (13)$$

References

- [1] Zhu, W., Dong, S.: Exoplanet Statistics and Theoretical Implications. *ARA&A* **59**, 291–336 (2021) <https://doi.org/10.1146/annurev-astro-112420-020055> [arXiv:2103.02127](https://arxiv.org/abs/2103.02127) [astro-ph.EP]
- [2] Pollack, J.B., Hubickyj, O., Bodenheimer, P., Lissauer, J.J., Podolak, M., Greenzweig, Y.: Formation of the Giant Planets by Concurrent Accretion of Solids and Gas. *Icarus* **124**(1), 62–85 (1996) <https://doi.org/10.1006/icar.1996.0190>
- [3] Ormel, C.W., Klahr, H.H.: The effect of gas drag on the growth of protoplanets. Analytical expressions for the accretion of small bodies in laminar disks. *A&A* **520**, 43 (2010) <https://doi.org/10.1051/0004-6361/201014903> [arXiv:1007.0916](https://arxiv.org/abs/1007.0916) [astro-ph.EP]
- [4] Lambrechts, M., Johansen, A.: Rapid growth of gas-giant cores by pebble accretion. *A&A* **544**, 32 (2012) <https://doi.org/10.1051/0004-6361/201219127> [arXiv:1205.3030](https://arxiv.org/abs/1205.3030) [astro-ph.EP]
- [5] Mayor, M., Queloz, D.: A Jupiter-mass companion to a solar-type star. *Nature* **378**(6555), 355–359 (1995) <https://doi.org/10.1038/378355a0>
- [6] Winn, J.N., Fabrycky, D.C.: The Occurrence and Architecture of Exoplanetary Systems. *ARA&A* **53**, 409–447 (2015) <https://doi.org/10.1146/annurev-astro-082214-122246> [arXiv:1410.4199](https://arxiv.org/abs/1410.4199) [astro-ph.EP]
- [7] Morales, J.C., Mustill, A.J., Ribas, I., Davies, M.B., Reiners, A., Bauer, F.F., Kossakowski, D., Herrero, E., Rodríguez, E., López-González, M.J., Rodríguez-López, C., Béjar, V.J.S., González-Cuesta, L., Luque, R., Pallé, E., Perger, M., Baroch, D., Johansen, A., Klahr, H., Mordasini, C., Anglada-Escudé, G.,

Caballero, J.A., Cortés-Contreras, M., Dreizler, S., Lafarga, M., Nagel, E., Passegger, V.M., Reffert, S., Rosich, A., Schweitzer, A., Tal-Or, L., Trifonov, T., Zechmeister, M., Quirrenbach, A., Amado, P.J., Guenther, E.W., Hagen, H.-J., Henning, T., Jeffers, S.V., Kaminski, A., Kürster, M., Montes, D., Seifert, W., Abellán, F.J., Abril, M., Aceituno, J., Aceituno, F.J., Alonso-Floriano, F.J., Ammler-von Eiff, M., Antona, R., Arroyo-Torres, B., Azzaro, M., Barrado, D., Becerril-Jarque, S., Benítez, D., Berdiñas, Z.M., Bergond, G., Brinkmüller, M., del Burgo, C., Burn, R., Calvo-Ortega, R., Cano, J., Cárdenas, M.C., Guillén, C.C., Carro, J., Casal, E., Casanova, V., Casasayas-Barris, N., Chaturvedi, P., Cifuentes, C., Claret, A., Colomé, J., Czesla, S., Díez-Alonso, E., Dorda, R., Emsenhuber, A., Fernández, M., Fernández-Martín, A., Ferro, I.M., Fuhrmeister, B., Galadí-Enríquez, D., Cava, I.G., Vargas, M.L.G., Garcia-Piquer, A., Gesa, L., González-Álvarez, E., Hernández, J.I.G., González-Peinado, R., Guàrdia, J., Guijarro, A., de Guindos, E., Hatzes, A.P., Hauschildt, P.H., Hedrosa, R.P., Hermelo, I., Arabi, R.H., Otero, F.H., Hintz, D., Holgado, G., Huber, A., Huke, P., Johnson, E.N., de Juan, E., Kehr, M., Kemmer, J., Kim, M., Klüter, J., Klutsch, A., Labarga, F., Labiche, N., Lalitha, S., Lampón, M., Lara, L.M., Launhardt, R., Lázaro, F.J., Lizon, J.-L., Llamas, M., Lodieu, N., López del Fresno, M., Salas, J.F.L., López-Santiago, J., Madinabeitia, H.M., Mall, U., Mancini, L., Mand el, H., Marfil, E., Molina, J.A.M., Martín, E.L., Martín-Fernández, P., Martín-Ruiz, S., Martínez-Rodríguez, H., Marvin, C.J., Mirabet, E., Moya, A., Naranjo, V., Nelson, R.P., Nortmann, L., Nowak, G., Ofir, A., Pascual, J., Pavlov, A., Pedraz, S., Medialdea, D.P., Pérez-Calpena, A., Perryman, M.A.C., Rabaza, O., Ballesta, A.R., Rebolo, R., Redondo, P., Rix, H.-W., Rodler, F., Trinidad, A.R., Sabotta, S., Sadegi, S., Salz, M., Sánchez-Blanco, E., Carrasco, M.A.S., Sánchez-López, A., Sanz-Forcada, J., Sarkis, P., Sarmiento, L.F., Schäfer, S., Schlecker, M., Schmitt, J.H.M.M., Schöfer, P., Solano, E., Sota, A., Stahl, O., Stock, S., Stuber, T., Stürmer, J., Suárez, J.C., Taberner, H.M., Tulloch, S.M., Veredas, G., Vico-Linares, J.I., Vilardell, F., Wagner, K., Winkler, J., Wolthoff, V., Yan, F., Osorio, M.R.Z.: A giant exoplanet orbiting a very-low-mass star challenges planet formation models. *Science* **365**(6460), 1441–1445 (2019) <https://doi.org/10.1126/science.aax3198> [arXiv:1909.12174](https://arxiv.org/abs/1909.12174) [astro-ph.EP]

- [8] Marois, C., Macintosh, B., Barman, T., Zuckerman, B., Song, I., Patience, J., Lafrenière, D., Doyon, R.: Direct Imaging of Multiple Planets Orbiting the Star HR 8799. *Science* **322**(5906), 1348 (2008) <https://doi.org/10.1126/science.1166585> [arXiv:0811.2606](https://arxiv.org/abs/0811.2606) [astro-ph]
- [9] Lafrenière, D., Jayawardhana, R., Janson, M., Helling, C., Witte, S., Hauschildt, P.: Discovery of an $\sim 23 M_{Jup}$ Brown Dwarf Orbiting ~ 700 AU from the Massive Star HIP 78530 in Upper Scorpius. *ApJ* **730**(1), 42 (2011) <https://doi.org/10.1088/0004-637X/730/1/42> [arXiv:1101.4666](https://arxiv.org/abs/1101.4666) [astro-ph.SR]
- [10] Miret-Roig, N., Bouy, H., Raymond, S.N., Tamura, M., Bertin, E., Barrado, D., Olivares, J., Galli, P.A.B., Cuillandre, J.-C., Sarro, L.M., Berihuete, A., Huélamo, N.: A rich population of free-floating planets in the Upper Scorpius

- young stellar association. *Nature Astronomy* **6**, 89–97 (2022) <https://doi.org/10.1038/s41550-021-01513-x> arXiv:2112.11999 [astro-ph.EP]
- [11] Pearson, S.G., McCaughrean, M.J.: Jupiter Mass Binary Objects in the Trapezium Cluster. arXiv e-prints, 2310–01231 (2023) <https://doi.org/10.48550/arXiv.2310.01231> arXiv:2310.01231 [astro-ph.EP]
- [12] Lin, D.N.C., Bodenheimer, P., Richardson, D.C.: Orbital migration of the planetary companion of 51 Pegasi to its present location. *Nature* **380**(6575), 606–607 (1996) <https://doi.org/10.1038/380606a0>
- [13] Winn, J.N., Fabrycky, D., Albrecht, S., Johnson, J.A.: Hot Stars with Hot Jupiters Have High Obliquities. *ApJ* **718**(2), 145–149 (2010) <https://doi.org/10.1088/2041-8205/718/2/L145> arXiv:1006.4161 [astro-ph.EP]
- [14] Chatterjee, S., Ford, E.B., Matsumura, S., Rasio, F.A.: Dynamical Outcomes of Planet-Planet Scattering. *ApJ* **686**(1), 580–602 (2008) <https://doi.org/10.1086/590227> arXiv:astro-ph/0703166 [astro-ph]
- [15] Lee, E.J.: The Boundary between Gas-rich and Gas-poor Planets. *ApJ* **878**(1), 36 (2019) <https://doi.org/10.3847/1538-4357/ab1b40> arXiv:1904.10470 [astro-ph.EP]
- [16] Lambrechts, M., Johansen, A.: Forming the cores of giant planets from the radial pebble flux in protoplanetary discs. *A&A* **572**, 107 (2014) <https://doi.org/10.1051/0004-6361/201424343> arXiv:1408.6094 [astro-ph.EP]
- [17] Boss, A.P.: Giant planet formation by gravitational instability. *Science* **276**, 1836–1839 (1997) <https://doi.org/10.1126/science.276.5320.1836>
- [18] Gammie, C.F.: Nonlinear Outcome of Gravitational Instability in Cooling, Gaseous Disks. *ApJ* **553**(1), 174–183 (2001) <https://doi.org/10.1086/320631> arXiv:astro-ph/0101501 [astro-ph]
- [19] Rafikov, R.R.: Can Giant Planets Form by Direct Gravitational Instability? *ApJ* **621**(1), 69–72 (2005) <https://doi.org/10.1086/428899> arXiv:astro-ph/0406469 [astro-ph]
- [20] Boley, A.C., Durisen, R.H.: On the Possibility of Enrichment and Differentiation in Gas Giants During Birth by Disk Instability. *ApJ* **724**(1), 618–639 (2010) <https://doi.org/10.1088/0004-637X/724/1/618> arXiv:1005.2624 [astro-ph.EP]
- [21] Nayakshin, S.: Formation of terrestrial planet cores inside giant planet embryos. *MNRAS* **413**(2), 1462–1478 (2011) <https://doi.org/10.1111/j.1365-2966.2011.18230.x> arXiv:1007.4165 [astro-ph.EP]
- [22] Zhu, Z., Hartmann, L., Nelson, R.P., Gammie, C.F.: Challenges in Forming

Planets by Gravitational Instability: Disk Irradiation and Clump Migration, Accretion, and Tidal Destruction. *ApJ* **746**(1), 110 (2012) <https://doi.org/10.1088/0004-637X/746/1/110> arXiv:1111.6943 [astro-ph.SR]

- [23] Keppler, M., Benisty, M., Müller, A., Henning, T., van Boekel, R., Cantalloube, F., Ginski, C., van Holstein, R.G., Maire, A.-L., Pohl, A., Samland, M., Avenhaus, H., Baudino, J.-L., Boccaletti, A., de Boer, J., Bonnefoy, M., Chauvin, G., Desidera, S., Langlois, M., Lazzoni, C., Marleau, G.-D., Mordasini, C., Pawellek, N., Stolker, T., Vigan, A., Zurlo, A., Birnstiel, T., Brandner, W., Feldt, M., Flock, M., Girard, J., Gratton, R., Hagelberg, J., Isella, A., Janson, M., Juhasz, A., Kemmer, J., Kral, Q., Lagrange, A.-M., Launhardt, R., Matter, A., Ménard, F., Milli, J., Mollière, P., Olofsson, J., Pérez, L., Pinilla, P., Pinte, C., Quanz, S.P., Schmidt, T., Udry, S., Wahhaj, Z., Williams, J.P., Buenzli, E., Cudel, M., Dominik, C., Galicher, R., Kasper, M., Lannier, J., Mesa, D., Mouillet, D., Peretti, S., Perrot, C., Salter, G., Sissa, E., Wildi, F., Abe, L., Antichi, J., Augereau, J.-C., Baruffolo, A., Baudoz, P., Bazzon, A., Beuzit, J.-L., Blanchard, P., Brems, S.S., Buey, T., De Caprio, V., Carbillet, M., Carle, M., Cascone, E., Cheetham, A., Claudi, R., Costille, A., Delboulbé, A., Dohlen, K., Fantinel, D., Feautrier, P., Fusco, T., Giro, E., Gluck, L., Gry, C., Hubin, N., Hugot, E., Jaquet, M., Le Mignant, D., Llored, M., Madec, F., Magnard, Y., Martinez, P., Maurel, D., Meyer, M., Möller-Nilsson, O., Moulin, T., Mugnier, L., Origné, A., Pavlov, A., Perret, D., Petit, C., Pragt, J., Puget, P., Rabou, P., Ramos, J., Rigal, F., Rochat, S., Roelfsema, R., Rousset, G., Roux, A., Salasnich, B., Sauvage, J.-F., Sevin, A., Soenke, C., Stadler, E., Suarez, M., Turatto, M., Weber, L.: Discovery of a planetary-mass companion within the gap of the transition disk around PDS 70. *A&A* **617**, 44 (2018) <https://doi.org/10.1051/0004-6361/201832957> arXiv:1806.11568 [astro-ph.EP]
- [24] Haffert, S.Y., Bohn, A.J., de Boer, J., Snellen, I.A.G., Brinchmann, J., Girard, J.H., Keller, C.U., Bacon, R.: Two accreting protoplanets around the young star PDS 70. *Nature Astronomy* **3**, 749–754 (2019) <https://doi.org/10.1038/s41550-019-0780-5> arXiv:1906.01486 [astro-ph.EP]
- [25] Laughlin, G., Adams, F.C.: The Modification of Planetary Orbits in Dense Open Clusters. *ApJ* **508**(2), 171–174 (1998) <https://doi.org/10.1086/311736>
- [26] Bonnell, I.A., Smith, K.W., Davies, M.B., Horne, K.: Planetary dynamics in stellar clusters. *MNRAS* **322**(4), 859–865 (2001) <https://doi.org/10.1046/j.1365-8711.2001.04171.x> arXiv:astro-ph/0012020 [astro-ph]
- [27] Ford, E.B., Rasio, F.A., Yu, K.: Chaotic Interactions in Multiple Planet Systems. *ISSI Scientific Reports Series* **6**, 123–136 (2006)
- [28] Malmberg, D., de Angeli, F., Davies, M.B., Church, R.P., Mackey, D., Wilkinson, M.I.: Close encounters in young stellar clusters: implications for planetary systems in the solar neighbourhood. *MNRAS* **378**(3), 1207–1216 (2007) <https://doi.org/10.1111/j.1365-2966.2007.11885.x> arXiv:astro-ph/0702524 [astro-ph]

- [29] Fregeau, J.M., Chatterjee, S., Rasio, F.A.: Dynamical Interactions of Planetary Systems in Dense Stellar Environments. *ApJ* **640**(2), 1086–1098 (2006) <https://doi.org/10.1086/500111> arXiv:astro-ph/0510748 [astro-ph]
- [30] Malmberg, D., Davies, M.B., Heggie, D.C.: The effects of fly-bys on planetary systems. *MNRAS* **411**(2), 859–877 (2011) <https://doi.org/10.1111/j.1365-2966.2010.17730.x> arXiv:1009.4196 [astro-ph.EP]
- [31] Hao, W., Kouwenhoven, M.B.N., Spurzem, R.: The dynamical evolution of multiplanet systems in open clusters. *MNRAS* **433**(1), 867–877 (2013) <https://doi.org/10.1093/mnras/stt771> arXiv:1305.1413 [astro-ph.EP]
- [32] Shara, M.M., Hurley, J.R., Mardling, R.A.: Dynamical Interactions Make Hot Jupiters in Open Star Clusters. *ApJ* **816**(2), 59 (2016) <https://doi.org/10.3847/0004-637X/816/2/59> arXiv:1411.7061 [astro-ph.EP]
- [33] Cai, M.X., Kouwenhoven, M.B.N., Portegies Zwart, S.F., Spurzem, R.: Stability of multiplanetary systems in star clusters. *MNRAS* **470**(4), 4337–4353 (2017) <https://doi.org/10.1093/mnras/stx1464> arXiv:1706.03789 [astro-ph.EP]
- [34] Flammini Dotti, F., Kouwenhoven, M.B.N., Cai, M.X., Spurzem, R.: Planetary systems in a star cluster I: the Solar system scenario. *MNRAS* **489**(2), 2280–2297 (2019) <https://doi.org/10.1093/mnras/stz2346> arXiv:1908.07747 [astro-ph.EP]
- [35] Fragione, G.: Dynamical origin of S-type planets in close binary stars. *MNRAS* **483**(3), 3465–3471 (2019) <https://doi.org/10.1093/mnras/sty3367> arXiv:1812.02754 [astro-ph.EP]
- [36] Li, D., Mustill, A.J., Davies, M.B.: Fly-by encounters between two planetary systems I: Solar system analogues. *MNRAS* **488**(1), 1366–1376 (2019) <https://doi.org/10.1093/mnras/stz1794> arXiv:1902.09804 [astro-ph.EP]
- [37] Wang, Y.-H., Perna, R., Leigh, N.W.C.: Planetary architectures in interacting stellar environments. *MNRAS* **496**(2), 1453–1470 (2020) <https://doi.org/10.1093/mnras/staa1627> arXiv:2002.05727 [astro-ph.EP]
- [38] Wang, Y.-H., Perna, R., Leigh, N.W.C.: Giant Planet Swaps during Close Stellar Encounters. *ApJ* **891**(1), 14 (2020) <https://doi.org/10.3847/2041-8213/ab77d0> arXiv:2002.08366 [astro-ph.EP]
- [39] Li, D., Mustill, A.J., Davies, M.B.: Flyby encounters between two planetary systems II: exploring the interactions of diverse planetary system architectures. *MNRAS* **496**(2), 1149–1165 (2020) <https://doi.org/10.1093/mnras/staa1622> arXiv:2002.09271 [astro-ph.EP]
- [40] Moore, N.W.H., Li, G., Adams, F.C.: Inclination Excitation of Solar System Debris Disk Due to Stellar Flybys. *ApJ* **901**(2), 92 (2020) <https://doi.org/10.3847/2041-8213/ab77d0>

[3847/1538-4357/abb08f](https://doi.org/10.3847/1538-4357/abb08f) [arXiv:2007.15666](https://arxiv.org/abs/2007.15666) [astro-ph.EP]

- [41] Wang, Y.-H., Leigh, N.W.C., Perna, R., Shara, M.M.: Hot Jupiter and Ultra-cold Saturn Formation in Dense Star Clusters. *ApJ* **905**(2), 136 (2020) <https://doi.org/10.3847/1538-4357/abc619> [arXiv:2011.01236](https://arxiv.org/abs/2011.01236) [astro-ph.EP]
- [42] Carter, E.J., Stamatellos, D.: On the survivability of a population of gas giant planets on wide orbits. *MNRAS* **525**(2), 1912–1921 (2023) <https://doi.org/10.1093/mnras/stad2314> [arXiv:2307.14908](https://arxiv.org/abs/2307.14908) [astro-ph.EP]
- [43] Heggie, D.C.: Binary evolution in stellar dynamics. *MNRAS* **173**, 729–787 (1975) <https://doi.org/10.1093/mnras/173.3.729>
- [44] Hut, P., Bahcall, J.N.: Binary-single star scattering. I - Numerical experiments for equal masses. *ApJ* **268**, 319–341 (1983) <https://doi.org/10.1086/160956>
- [45] Sigurdsson, S., Phinney, E.S.: Binary–Single Star Interactions in Globular Clusters. *ApJ* **415**, 631 (1993) <https://doi.org/10.1086/173190>
- [46] Mathieu, R.D.: Pre-Main-Sequence Binary Stars. *ARA&A* **32**, 465–530 (1994) <https://doi.org/10.1146/annurev.aa.32.090194.002341>
- [47] Raghavan, D., McAlister, H.A., Henry, T.J., Latham, D.W., Marcy, G.W., Mason, B.D., Gies, D.R., White, R.J., ten Brummelaar, T.A.: A Survey of Stellar Families: Multiplicity of Solar-type Stars. *ApJS* **190**(1), 1–42 (2010) <https://doi.org/10.1088/0067-0049/190/1/1> [arXiv:1007.0414](https://arxiv.org/abs/1007.0414) [astro-ph.SR]
- [48] Nielsen, E.L., De Rosa, R.J., Macintosh, B., Wang, J.J., Ruffio, J.-B., Chiang, E., Marley, M.S., Saumon, D., Savransky, D., Ammons, S.M., Bailey, V.P., Barman, T., Blain, C., Bulger, J., Burrows, A., Chilcote, J., Cotten, T., Czekala, I., Doyon, R., Duchêne, G., Esposito, T.M., Fabrycky, D., Fitzgerald, M.P., Follette, K.B., Fortney, J.J., Gerard, B.L., Goodsell, S.J., Graham, J.R., Greenbaum, A.Z., Hibon, P., Hinkley, S., Hirsch, L.A., Hom, J., Hung, L.-W., Dawson, R.I., Ingraham, P., Kalas, P., Konopacky, Q., Larkin, J.E., Lee, E.J., Lin, J.W., Maire, J., Marchis, F., Marois, C., Metchev, S., Millar-Blanchaer, M.A., Morzinski, K.M., Oppenheimer, R., Palmer, D., Patience, J., Perrin, M., Poyneer, L., Pueyo, L., Rafikov, R.R., Rajan, A., Rameau, J., Rantakyrö, F.T., Ren, B., Schneider, A.C., Sivaramakrishnan, A., Song, I., Soummer, R., Tallis, M., Thomas, S., Ward-Duong, K., Wolff, S.: The Gemini Planet Imager Exoplanet Survey: Giant Planet and Brown Dwarf Demographics from 10 to 100 au. *AJ* **158**(1), 13 (2019) <https://doi.org/10.3847/1538-3881/ab16e9> [arXiv:1904.05358](https://arxiv.org/abs/1904.05358) [astro-ph.EP]
- [49] Vigan, A., Fontanive, C., Meyer, M., Biller, B., Bonavita, M., Feldt, M., Desidera, S., Marleau, G.-D., Emsenhuber, A., Galicher, R., Rice, K., Forgan, D., Morasini, C., Gratton, R., Le Coroller, H., Maire, A.-L., Cantalloube, F., Chauvin, G., Cheetham, A., Hagelberg, J., Lagrange, A.-M., Langlois, M., Bonnefoy, M., Beuzit, J.-L., Boccaletti, A., D’Orazi, V., Delorme, P., Dominik, C., Henning, T.,

Janson, M., Lagadec, E., Lazzoni, C., Ligi, R., Menard, F., Mesa, D., Messina, S., Moutou, C., Müller, A., Perrot, C., Samland, M., Schmid, H.M., Schmidt, T., Sissa, E., Turatto, M., Udry, S., Zurlò, A., Abe, L., Antichi, J., Asensio-Torres, R., Baruffolo, A., Baudoz, P., Baudrand, J., Bazzon, A., Blanchard, P., Bohn, A.J., Brown Sevilla, S., Carbillet, M., Carle, M., Cascone, E., Charton, J., Claudi, R., Costille, A., De Caprio, V., Delboulb e, A., Dohlen, K., Engler, N., Fantinel, D., Feautrier, P., Fusco, T., Gigan, P., Girard, J.H., Giro, E., Gisl er, D., Gluck, L., Gry, C., Hubin, N., Hugot, E., Jaquet, M., Kasper, M., Le Mignant, D., Llored, M., Madec, F., Magnard, Y., Martinez, P., Maurel, D., M oller-Nilsson, O., Mouillet, D., Moulin, T., Orign e, A., Pavlov, A., Perret, D., Petit, C., Pragt, J., Puget, P., Rabou, P., Ramos, J., Rickman, E.L., Rigal, F., Rochat, S., Roelfsema, R., Rousset, G., Roux, A., Salasnich, B., Sauvage, J.-F., Sevin, A., Soenke, C., Stadler, E., Suarez, M., Wahhaj, Z., Weber, L., Wildi, F.: The SPHERE infrared survey for exoplanets (SHINE). III. The demographics of young giant exoplanets below 300 au with SPHERE. *A&A* **651**, 72 (2021) <https://doi.org/10.1051/0004-6361/202038107> arXiv:2007.06573 [astro-ph.EP]

- [50] Hillenbrand, L.A., Hartmann, L.W.: A Preliminary Study of the Orion Nebula Cluster Structure and Dynamics. *ApJ* **492**(2), 540–553 (1998) <https://doi.org/10.1086/305076>
- [51] Wang, Y.-H., Leigh, N.W.C., Liu, B., Perna, R.: SpaceHub: A high-performance gravity integration toolkit for few-body problems in astrophysics. *MNRAS* **505**(1), 1053–1070 (2021) <https://doi.org/10.1093/mnras/stab1189> arXiv:2104.06413 [astro-ph.SR]